Colloid Polym Sci (2004) 282: 351–356
DOI 10.1007/s00396-003-0942-x

ORIGINAL CONTRIBUTION

A. González-Pérez
J.M. Ruso
G. Prieto
F. Sarmiento

Physicochemical study of ovalbumin in the presence of sodium dodecyl sulphate in aqueous media

Received: 7 February 2003
Accepted: 26 May 2003
Published online: 13 August 2003

A. González-Pérez · J.M. Ruso (✉)
G. Prieto · F. Sarmiento
Biophysics and Interfaces Group,
Department of Applied Physics,
Faculty of Physics,
University of Santiago de Compostela,
15782 Santiago de Compostela, Spain
E-mail: faruso@usc.es
Tel.: +34-981-563100
Fax: +34-981-520676

Abstract The interactions of sodium dodecyl sulphate with ovalbumin in aqueous solution at room temperature are described for a wide concentration range of both substances. A phase diagram covering a wide range of concentrations shows a total of five different morphologies. Dynamic light scattering of the samples from each morphology offered better understanding of the different structures (between three and four) present in the solution. The amount of ovalbumin present in the solution was confirmed with differential scanning spectroscopy, while the interactions between sodium dodecyl sulphate and ovalbumin were interpreted by zeta potential and electrical conductivity measurements.

Keywords Ovalbumin · Sodium dodecyl sulphate · Phase diagram · Interactions

Introduction

Interaction of proteins with surfactants is of great importance in the fields of industrial (cosmetic, paints, food), biological and pharmaceutical sciences. Owing to the existence of nonpolar and ionic amino acid side chains in protein molecules, the formations of these complexes is driven by electrostatic interactions between the charged headgroups of the surfactants and the oppositely charged units of the proteins, as well as by hydrophobic interactions between the alkyl chains and different parts of the proteins [1, 2].

Ovalbumin, a major component of egg white proteins, is grouped into family serine proteinase inhibitors, which control serine proteinases involved in diverse physiological reactions, because of the close similarity in the primary and tertiary structures. It has a molecular weight of 45,000 and consists of a single chain of 385 amino acid residues, with a total of 105 titrable residues [3], contains a single disulphide bond (interconnecting two parts of the chain) and a glycosylation (manly mannose) site. Three different phosphate forms of ovalbumin occur in egg white, containing two, one or no phosphate groups per molecule. Typically, in egg white, the ratios of each are about 85:12:3 [4]. This protein has a globular shape with a radius of around 3 nm in an aqueous medium and an isoelectric point at pH 4.6 [4]. When stored for extended periods of time, or by heat processing, the native *R* form of ovalbumin converts to *S*-ovalbumin, which is more resistant to denaturation by heat, urea, or guanidine [5].

The ovalbumin globules are also known to make a self-organized mesoscopic structure, which is governed by several factors: temperature, concentration, electrolyte, etc [6]. As a result, solutes are often added to regulate these transformations during the processing of proteins or proteins-containing food materials. To effectively control and optimize this food processing, a broad understanding of how added solutes influence protein morphology is essential.

In the present study, we investigated the effect of a typical anionic surfactant, sodium dodecyl sulphate

(SDS), on the structure of the ovalbumin solution. For this purpose several samples, covering a wide range of concentrations of protein and surfactant, were prepared. The physicochemical properties of these samples were evaluated by using several experimental techniques: electrical conductivity, zeta potential and difference spectroscopy.

Experimental

Materials

Ovalbumin (albumin, chicken egg, product A-5,253, Sigma Chemical Company) was used without further purification. SDS (product 5,987) was obtained from Lancaster MTM Research Chemicals. All materials were of analytical grade and solutions were made in double-distilled water.

Conductivity

Conductance was measured using a conductivity meter (Kyoto Electronics type C-117), the cell of which (Kyoto, type K-121) was calibrated with KCl solutions in the appropriate concentration range. The cell constant was calculated using molar conductivity data published by Shedlovsky [7] and Chambers et al. [8]. Water was progressively added to a concentrated aqueous solution of surfactant and surfactant plus protein, respectively, of known concentration and composition using a peristaltic pump (Dosimat, model-655, Metrohm) under the control of a Hewlett-Packard Vectra computer. The measuring cell was immersed in a Polyscience PS9105 thermostatted bath, which maintained the temperature constant to within ± 0.01 K. The duration of dynamical processes may vary from 10^{-8} (which is the time it takes a surfactant to leave or enter a micelle) to 10^{-2} (the time scale of the fusion of micelles) [9], so the equilibrium process is guaranteed in just a few seconds after dilution when the measurement is made.

Dynamic light scattering

Dynamic light scattering measurements were made at 298 ± 0.1 K and at a scattering angle of 90° using an Coherent DPSS 532 laser light scattering instrument equipped with a 0.5-W solid-state laser, operating at 532 nm with vertically polarized light. Time correlation was analyzed by an ALV-5000 multiple-τ correlator (ALV, Langen, Germany). Diffusion coefficients were determined from a single-exponential fit to the correlation curve. Hydrodynamic radii were calculated from measured diffusion coefficients by means of the Stokes–Einstein equation.

Zeta potential

Zeta potentials of the SDS–ovalbumin complexes were measured using a Malvern Instruments Zetamaster 5002 by taking the average of five measurements at stationary level. The cell used was a 5 mm×2 mm rectangular quartz capillary. The temperature of the experiments was 298.15 ± 0.01 K and was controlled by a HETO proportional temperature controller. The zeta potential were calculated from the electrophoretic mobilities, μ_E, using the Henry equation:

$$\zeta = \frac{3\mu_E \eta}{2\varepsilon_0 \varepsilon_r} \frac{1}{f(\kappa a)}, \quad (1)$$

where ε_0 is the permittivity of a vacuum, ε_r is the relative permittivity, a is the particle radius, κ is the Debye length and η is the viscosity of water. The function $f(\kappa a)$ depends on the particle shape and for our system was determined by

$$f(\kappa a) = \frac{3}{2} - \frac{9}{2\kappa a} + \frac{75}{2\kappa^2 a^2} - \frac{330}{\kappa^3 a^3}, \quad (2)$$

which is valid for $\kappa a > 1$.

Spectroscopy

Difference spectra were measured using a Beckman spectrophotometer (model DU 640), with six microcuvettes, operating in the UV–vis region, with a full-scale expansion of 0.2 absorbance units. For absorbance difference spectra, five of the six microcuvettes were filled with protein plus surfactant solutions. The first microcuvette contained only protein in the corresponding medium and was used as a blank reference. The microcuvettes were filled and placed in the same orientation for all the tests. The absorbance was measured at 298.15 ± 0.01 K using a temperature controller (Beckman DU series), based on the Peltier effect.

Results and discussion

All samples were made up by weight in duplicate. Since the morphology obtained was sometimes dependent on the sequence of addition, the components were always added in the following order: water, protein and SDS. High concentration increments were initially used to identify the general morphology regions; however, when a phase change was observed for one solution to the next, solutions in this concentration range were then prepared with low increments to delineate the precise phase boundary. The morphology of each sample at room temperature was determined by visual observation by two observers. All the samples were made in duplicate to verify the morphologies observed. After examining all samples, a total of five morphologies could be distinguished visually (Fig. 1, Table 1).

At ovalbumin concentrations below 0.34% and 0.14% SDS the samples were a transparent, colourless liquid with small particles in suspension (morphology I). An increase in SDS or ovalbumin results in morphologies II or III, respectively. It is possible to observe a similar aspect in morphology II to that found in morphology I; however, a small soft hydrated gel instead of the small particles could be observed. Visual inspection of morphology III shows the appearance of a few white precipitates and an increase in the viscosity of the samples, but they are still transparent. No particles or soft gel in solution are present. Further addition of ovalbumin and SDS in concentrations below 0.5% will drive, firstly, morphology IV turbid and with a great amount of precipitate (3 times larger than found in the previous

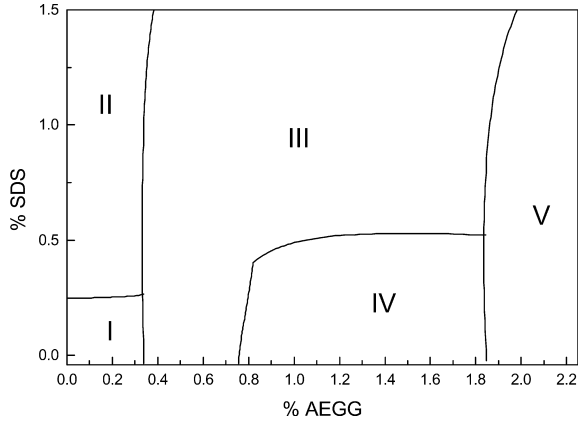

Fig. 1 Phase diagram of the ovalbumin (*AEGG*)–sodium dodecyl sulphate (*SDS*) system

morphology) and, secondly, morphology V (above 1.84% ovalbumin), turbid, yellow and with less precipitate than morphology IV. However there is a direct way from morphology III to morphology V; this is for SDS concentrations over 0.5%.

Previous studies have shown changes in the morphologies of ovalbumin in ammonia [10], ethanol [11] and sodium chloride [12] solutions or the effect of heating [13, 14], and the morphologies were close to those found in this study. Aoki and coworkers [15, 16, 17, 18] studied the interaction of SDS with ovalbumin in acetate buffer solution at pH 4.2, and found that the amount of precipitate formed changed with the mixing ratio of ovalbumin to SDS from a large amount of white precipitate when albumin is in excess (this amount presents a gradual decrease with an increase in the relative amount of SDS) to a region of no precipitate when the relative amount of SDS exceed a mixing ratio of 45:55. A similar result was obtained in our study; the precipitate appears and increases with protein concentrations. In morphology IV a great amount of precipitate could be observed owing to the lower concentration of SDS in this area (in area III over area IV the SDS concentration is higher, keeping the mixing ratio low).

Table 1 Ovalbumin–sodium dodecyl sulphate (*SDS*) phase diagram morphology descriptions

Morphology	Description
I	Transparent liquid, clear and colourless with small particles in suspension
II	Transparent liquid, clear and colourless with a soft hydrated gel
III	Transparent liquid, clear and colourless with little precipitate
IV	Turbid liquid, colourless with a great amount of precipitate
V	Turbid liquid, yellow with precipitate

Aoki [16] found that precipitation occurs when the anionic surfactant and the protein are mixed at a lower pH that than of the isoelectric point of the protein, while no precipitation occurs at a pH above the isoelectric point. This study was realized to low protein concentrations (keeping the sum of the concentration of SDS and that of egg albumin constant at 1%). We checked the pH of all the samples in the range 7.5–8.0, which guaranties that the protein is above its isoelectric point, i.e., no precipitation occurs. However this fact is only true for lower protein concentrations, so the precipitate begins to appear in morphology III, increasing the amount of precipitate in morphologies IV and V.

For better and deeper understanding of these morphologies, dynamic light scattering was employed. We prepared samples covering not only all morphologies but in the case of morphologies III and V, which cover areas above and below the SDS critical micelle concentration (cmc), both regions were studied as well. The size distribution of the samples for different ovalbumin concentrations and SDS concentrations below and above the cmc are shown in Figs. 2 and 3, respectively. The size distribution plots are large and heterogeneous. In Fig. 2 three peaks can be observed around 3, 40 and 550 nm. The first peak tends to decrease, while the others grow when the protein concentration rises. The first peak corresponds to individual protein molecules, which are not linked to the intermediate and large structures (40 and 550-nm peaks). A similar size distribution was found for only ovalbumin (8.0% in 10 mM phosphate buffer) [19] with broad peaks for the intermediate and large structures formed by a gel protein

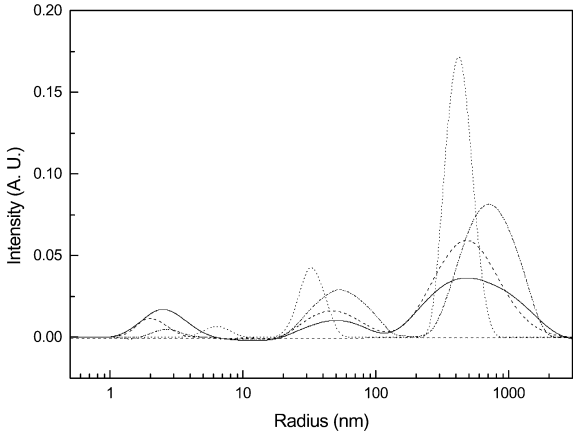

Fig. 2 Particle size distribution for different AEGG concentrations and SDS concentrations below the critical micelle concentration (*cmc*): the *solid line* corresponds to morphology I (0.18% AEGG, 0.07% SDS); the *dashed line* corresponds to morphology III (0.66% AEGG, 0.07% SDS); the *dash-dotted line* corresponds to morphology IV (1.43% AEGG, 0.07% SDS); and the *dotted line* corresponds to morphology V (2.09% AEGG, 0.07% SDS)

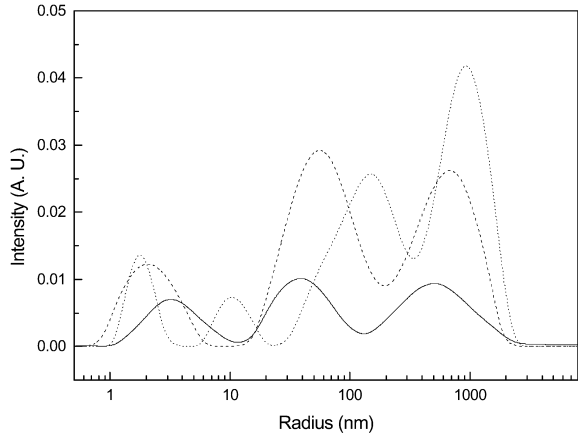

Fig. 3 Particle size distribution for different AEGG concentrations and SDS concentrations above the cmc: the *solid line* corresponds to morphology II (0.18% AEGG, 0.72% SDS); the *dashed line* corresponds to morphology III (1.43% AEGG, 0.72% SDS); and the *dotted line* corresponds to morphology V (2.09% AEGG, 0.72% SDS)

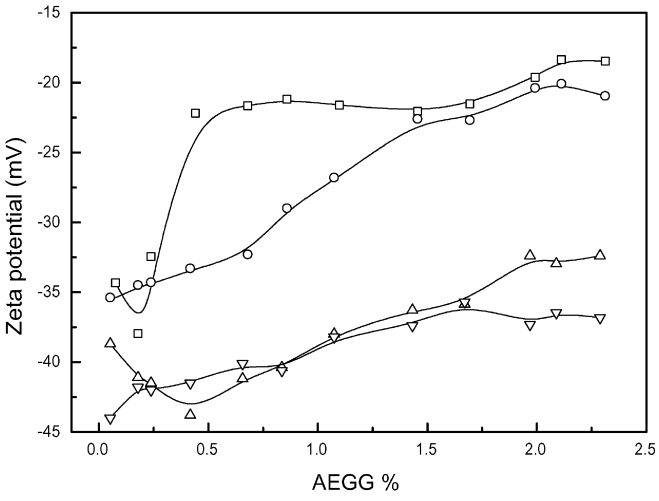

Fig. 4 Zeta potential as a function of AEGG concentration in aqueous solutions of SDS concentrations of 0.07% (*squares*), 0.15% (*circles*), 0.72% (*up triangles*) and 1.44% (*down triangles*)

matrix. Interaction of SDS with proteins begins at low concentrations and can increase to form clusters over the protein at high surfactant concentrations [20, 21], so it could be expected that surfactant molecules are present in all the structures. The increase in protein concentration leads to a diminution of the smaller peak and a rise of the bigger ones. The size distribution for SDS concentrations above the cmc is shown in Fig. 3; now only three morphologies are present: II, III and V. Again three peaks are present, except for morphology V, where a fourth peak appears. The peak is centred relatively close to those shown in Fig. 2, but with a broader distribution. The same pattern can be observed, a decrease in the smaller one and an increase in the others. The presence of SDS micelles cannot be observed in these plots, probably owing to their closeness to the smaller peak. Inspection of both figures seems to indicate that the SDS concentration does not affect strongly the morphology of the system.

Zeta potential measurements of some samples are shown in Fig. 4. For each plot we kept the SDS concentration constant; two plots are below and two are above the SDS cmc, while the ovalbumin concentration was changing. Thus we have four ways crossing horizontally (Fig. 1). Two main features can be obtained from these plots. First, an increase in SDS concentration tends to a more negative charge of the particles, i.e., more SDS molecules are adsorbed onto the protein. Second, plots corresponding to SDS concentrations below the cmc exhibit more drastic changes in the zeta potential than those for concentration above the cmc, where the plots are smoother. These leaps correlate with changes from morphology I to morphology III, while above the cmc, changes from morphologies II to III are smoother. On the other hand it is clear that SDS begins to interact with egg albumin at very low concentrations, because Sengupta et al. [22] found zeta potential values for egg albumin in water of −8.5 mV. It is well known that the formation of protein surfactant complexes is driven by electrostatic interactions between the charged headgroup of the surfactants and the oppositely charged units of the protein, as well as by hydrophobic interactions between the alkyl chain of the surfactants and the nonpolar protein residues. In aqueous media surfactants ions compete with water molecules for binding sites on the protein, for which in the case of egg albumin Bull and Breese [23] found an average number of 33 mol water bound per mole of ovalbumin [23]. However in this case the adsorption is mainly driven by hydrophobic interactions due to the protein and the surfactant presents the same charge.

The difference spectra in the wavelength range 260–380 nm are shown in Fig. 5. Addition of egg albumin results in the development of a positive absorption band at 280 nm, positive with respect to native egg albumin. In the inset we show the difference spectra obtained when keeping the ovalbumin concentration constant and changing the SDS concentration; it shows a decrease in the absorption when the SDS concentration increases, and the same result was verified in other areas. Such diminution of the protein concentration in solution is attributed to the precipitation, which is induced by the presence of SDS. This result correlates well with the higher amount of precipitate found at the top areas of each morphology with reference to the bottom.

Continuing with our interest in the interactions between SDS, electrical conductivity measurements of SDS with different protein concentration (0.0, 0.1, 0.2 and

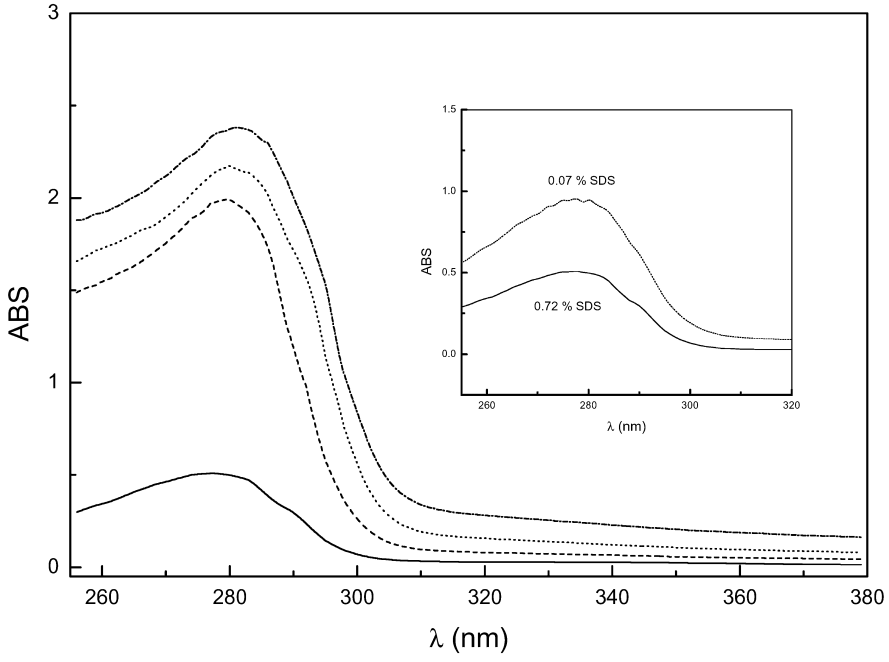

Fig. 5 Difference spectra of AEGG in the presence of SDS relative to native AEGG in water. The SDS concentration was 0.72% and the protein concentrations were 0.18% (*solid line*), 0.66% (*dashed line*), 1.43% (*dotted line*) and 2.09% (*dash-dotted line*). The *inset* shows the difference spectra for an AEGG concentration of 0.18% and a SDS concentration of 0.72% (*solid line*) and 0.07% (*dashed line*)

0.5%) solutions were measured in water at 298.15 K. Plots of the molal conductivity of the ovalbumin–SDS systems minus the molal conductivity of ovalbumin are shown in Fig. 6 as a function of the square root of the SDS molality. The breakpoints in the slopes of the plots were identified with the cmc of SDS; the numerical values are listed in Table 2. A clear increase in the cmc of SDS with protein concentration can be observed; such an event arises from the fact that SDS molecules are adsorbed on the protein surface, diminishing the number of monomers in solution and consistently the cmc is reached at higher SDS concentrations. This kind of behaviour in a system with a surfactant and polyelectrolytes is very common [24, 25]. The degrees of ionization, α, obtained from the relation between the slopes above and below the cmc of the plots of the electrical conductivity against the SDS molal concentration are listed in Table 2 and show an increase with protein concentration. It is interesting to compare this result with the results obtained for SDS and trypsin system, a globular protein [26] where the cmc of SDS increases with trypsin concentration and the counterion binding $(1-\alpha)$ is a maximum for pure SDS, and in the presence of trypsin their values are lower than that of pure SDS although they show an increasing trend with increasing concentration of trypsin.

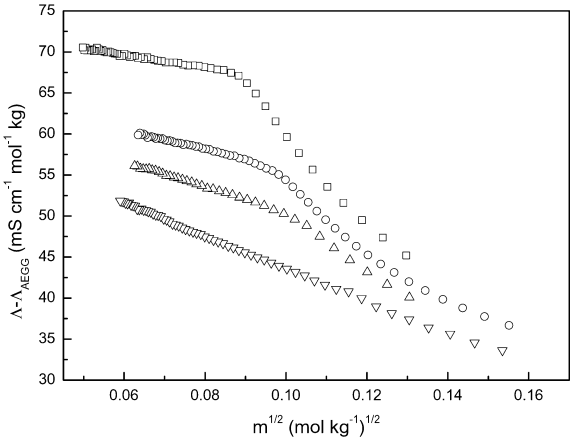

Fig. 6 Molal conductivity of the AEGG–SDS systems as a function of the square root of the SDS molality, for different protein concentrations: 0.0% (*squares*); 0.1% (*circles*); 0.2% (*up triangles*); and 0.5% (*down triangles*)

The number of SDS molecules adsorbed on the protein can be obtained from the conductivity plots, assuming that the displacement towards higher values of the SDS cmc is due to removal of surfactant molecules from the bulk solution to the surface of the protein. Thus the numbers of bound surfactant molecules per molecule of protein were found to be 57, 45 and 48 for ovalbumin concentration of 0.1, 0.2 and 0.5%, respec-

Table 2 Values of the critical micelle concentration (*cmc*) and degree of ionization, α, of SDS at different ovalbumin concentrations

Ovalbumin (%)	cmc ($\times 10^3$ mol kg^{-1})	α
0.0	8.24	0.36
0.1	9.51	0.44
0.2	10.24	0.50
0.5	13.55	0.75

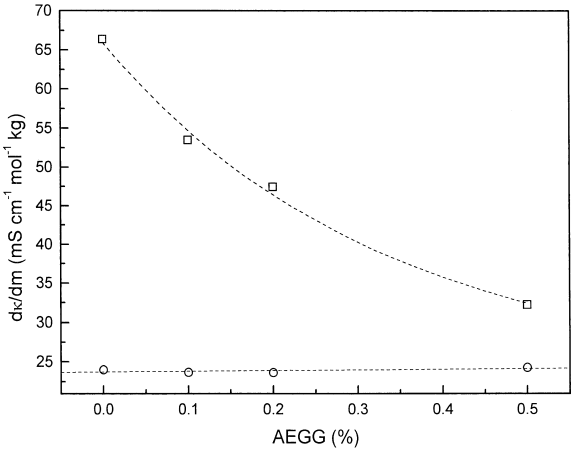

Fig. 7 Slope of the electrical conductivity against molality, below (*squares*) and above (*circles*) the SDS cmc, for different AEGG concentrations

tively. These numbers are of the same order as and are comparable with the average number of 40 found by Aoki et al. [17] in acetate buffer solution at pH 4.2.

Plots of the slopes of the electrical conductivity against molality, below and above the SDS cmc, are shown in Fig. 7 for different ovalbumin concentrations. Clearly the slope below the cmc decreases exponentially with protein concentration, while the slope above the cmc remain almost constant. The contribution to electrical conductivity of ovalbumin in solution increases linearly with protein concentration (with a slope of 1 mS cm^{-1} %$^{-1}$) so this behaviour could be attributed to the Na^+ ions of SDS which are adsorbed onto the protein by means of electrostatic interactions and releasing the water molecules on the surface.

Conclusions

In this study we analysed the behaviour and interactions in SDS plus egg albumin solutions over a wide concentration range. Five different morphologies were found by visual inspection. The other techniques employed offered us a better understanding of this system. Thus the presence of SDS micelles in solution will result in a wider size distribution of the structures. In mixtures containing two colloids of different size, the smaller one is excluded from the space between the surfaces of two nearby particles. This results in a net osmotic force pushing the particles together which can be modelled as an effective interparticle attraction, the depletion potential [27]. However, owing to the closer size between SDS micelles and protein particles, we believe that the interactions in this system are mainly driven by electrostatic and hydrophobic interactions. Interaction between SDS molecules and protein begin at low SDS concentrations, increasing the net negative charge of the protein. These interactions are driven by hydrophobic interactions, while from the conductivity study we can conclude that there is strong binding of Na^+ ions to ovalbumin driven by the electrostatic interactions. Finally, a total average number of 50 SDS molecules were found to bind to an ovalbumin molecule.

Acknowledgement A.G-P. thanks the University of Santiago de Compostela for a grant.

References

1. Jones MN (1988) In: Jones MN (ed) Biological thermodynamics. Elsevier, Amsterdam
2. Goddard ED (1986) Colloid Surf 19:301
3. Tatsumi E, Yoshimatsu D, Hirosi M (1998) Biochemistry 37:12351
4. Judge RA, Johns MR, White ET (1996) J Chem Eng Data 41:422
5. Egelandsdal B (1980) J Food Sci 44:1651
6. Sugiyama M, Nakamura A, Hiramatsu N, Annaka M, Kuwajima S, Hara K (2001) Biomacromolecules 2:1071
7. Shedlovsky T (1932) J Am Chem Soc 54:1411
8. Chambers JF, Stokes JM, Stokes RH (1956) J Phys Chem 60:985
9. Smit B, Essenlink K, Hilbers PAJ, van Os NM, Rupert LAM, Szeleifer I (1993) Langmuir 9:9
10. Judge RA, Johns MR, White ET (1996) J Chem Eng Data 41:422
11. Elysée-Collen B, Lencki, RW (1996) J Agric Food Chem 44:1658
12. Iametti S, Donnizzelli E, Pittia P, Rovere PP, Squarcina N, Bonomi F (1999) J Agric Food Chem. 47:3611
13. Mine Y (1996) J Agric Food Chem 44:2086
14. Sugiyama M, Nakamura A, Hiramatsu N, Annaka M, Kuwajima S, Hara K (2001) Biomacromolecules 2:1071
15. Aoki K, Hori J (1956) Bull Chem Soc Jpn 29:104
16. Aoki K (1956) Bull Chem Soc Jpn 29:369
17. Aoki K, Hori J, Sakurai, K (1956) Bull Chem Soc Jpn 29:758
18. Aoki K, Suzuki Y (1957) Bull Chem Soc Jpn 30:53
19. Mine Y (1996) J Agric Food Chem. 44:2086
20. Jones MN, Manley P (1984) In: Mittal KL, Lindman B (eds) Surfactants in solution. Plenum, London, pp
21. Goddard ED, Ananthapadmanabhan KP (eds) (1993) Interactions of surfactants with polymers and proteins. CRC, Boca Raton
22. Sengupta T, Razumovsky L, Damodaran S (1999) Langmuir 15:6991
23. Bull HB, Breese K (1976) Biopolymers 15:1573
24. Bakshi MS (2000) Colloid Polym Sci 278:524
25. Ruso JM, Sarmiento F (2000) Colloid Polym Sci 278:800
26. Ghosh S, Banerjee A (2002) Biomacromolecules 3:9
27. Petekidis G, Galloway LA, Egelhaaf SU, Cates ME, Poon WCK (2002) Langmuir 18:4248